Hyperfine Interact
DOI 10.1007/s10751-013-0977-4

Impact of active phase chemical composition and dispersity on catalytic behavior in PROX reaction

Z. Cherkezova-Zheleva · D. Paneva · S. Todorova · H. Kolev · M. Shopska · I. Yordanova · I. Mitov

Abstract Iron and iron-platinum catalysts supported on activated carbon have been successfully synthesized by wet impregnation method and low-temperature treatment in inert atmosphere. The content of the supported phases corresponds to 10 wt % Fe and 0.5 wt % Pt. Four catalytic samples were synthesized: Sample A—activated carbon impregnated with Fe nitrate; Sample B—activated carbon impregnated with Pt salt; Sample C—activated carbon impregnated consequently with Fe and Pt salts; Sample D—activated carbon impregnated simultaneously with Fe and Pt salts. The as-prepared materials were characterized by Mössbauer spectroscopy, X-ray diffraction, infrared and X-ray photoelectron spectroscopy. The spectra show that the activated carbon support and the preparation procedure give rise to the synthesis of isolated metal Pt ions and ultradispersed Fe and Pt oxide species. Probably the presence of different functional groups of activated carbon gives rise to registered very high dispersion of loaded species on support. The catalytic tests were carried out in PROX reaction. A lower activity of bimetallic Pt-Fe samples was explained with the increase in surface oxygen species as a result of predomination of iron oxide on the support leading to the increase in selectivity to the H_2 oxidation. Partial agglomeration of supported iron oxide phase was registered after catalytic tests.

Keywords Iron and iron-platinum catalysts · Activated carbon · XRD · Mössbauer spectroscopy · XPS · PROX

Proceedings of the 32nd International Conference on the Applications of the Mössbauer Effect (ICAME 2013) held in Opatija, Croatia, 1–6 September 2013.

Z. Cherkezova-Zheleva (✉) · D. Paneva · S. Todorova · H. Kolev · M. Shopska · I. Yordanova · I. Mitov
Institute of Catalysis, Bulgarian Academy of Sciences,
Acad. G. Bonchev Str., Bld. 11, Sofia 1113, Bulgaria
e-mail: zzhel@ic.bas.bg

Published online: 03 December 2013

1 Introduction

The PROX is a simple, efficient, and economic method for CO removal from hydrogen rich streams in comparison with other methods as membrane separation or pressure swing methods. The platinum is the most extensively studied metal for PROX reaction. The great disadvantage of the platinum catalysts is the metal loading, which currently is in the range of 2–6 wt.%. In view of the cost, it is preferable to reduce the metal content. The decrease in the reaction temperature and the search for more economic catalysts for selective CO oxidation are challenging objectives for the near future. The attempts have been made to improve the performance of platinum catalysts by the addition of promoters. In this regard, supported two component catalysts, incorporating more than one active component, may provide possibilities of synergism that lead to superior performance [1, 2].

The morphology and valence band structure of nano-sized (1–10 nm) metal and metal oxide particles differ fundamentally from those of the large particles in the terms of short-range ordering [3–11]. Their catalytic behaviour can be drastically changed due to its critically small particle size, based upon their new different magnetic, optic, electric, and other physicochemical properties. As far as iron oxide based systems are concerned, the formation of highly active site is associated with the formation of highly dispersed iron oxide and its optimal interaction with the support [3, 4, 8–10]. Ultrafine particles having nano-metric size can be prepared on different oxide supports, carbon supports, and in zeolites. The use of support decreases the content of active phases and also this prevents them from sintering. Carbon is a favourable support for making small supported iron particles having nano-metric size [8–10]. Porous carbon materials with varying structural and compositional properties are intensively studied to prepare highly active and selective catalysts for environmentally important and industrial chemical processes. The presented active centers on the surface of activated carbon took significant role on its technological applications. The research interest is also focused to look deeper insight into the preparation techniques of highly active and selective catalysts for a given reaction, i.e., what the factors are, that affect the genesis and stability of a highly active nano-sized particles giving rise to a good catalyst. These are the method and the conditions for precursor deposition, calcination, reduction, support pre-treatment, etc. The impregnation is a classical preparation method, but it has unused possibilities to prepare active phases in the nano-size region. Because of its simplicity and accessibility the method is not largely substituted by new techniques like laser ablation, “ion assisted” preparation (sol/gel techniques, sol precursors, zeolite encaged metal particles, etc.). It was shown that the activity of the supported catalysts differed significantly with the synthesis procedure. The catalysts prepared by incipient wetness impregnation are one of the most active. Probably the reason of different performance of the catalysts might be attributed to the different dispersity and crystallite size distribution, which would result in a variation of different phases presented in the catalyst under reaction conditions.

The aim of the present study was to investigate the influence of synthesis procedure and active phase chemical composition on the structure and dispersion in series of one- (Fe or Pt) and two-component (Fe-Pt) supported catalysts, containing nano-sized particles. Their behavior in PROX reaction and the existence of size-dependent effects were also studied.

2 Experimental

2.1 Catalyst preparation

Iron and iron-platinum catalysts supported on activated carbon were synthesized by wet impregnation method using solutions of $Fe(NO_3)_3 \cdot 9H_2O$ or/and Pt $(NH_3)_4Cl_2$. The activated carbon is prepared in the Trayal Corporation, Krushevac, by the water vapour activation of a mixture of a coal and anthracite at 1273 K [12].

The prepared samples are heated in inert atmosphere at 350 ^oC for 3 h. The content of the supported phases corresponds to 10 wt % Fe and 0.5 wt % Pt. Four catalytic samples were synthesized: **Sample A**—activated carbon impregnated with Fe nitrate; **Sample B**—activated carbon impregnated with Pt salt; **Sample C**—activated carbon impregnated consequently with Fe and Pt salts; **Sample D**—activated carbon impregnated simultaneously with Fe and Pt salts.

2.2 Physicochemical characterization

The phase composition and dispersity of materials were studied by Mössbauer spectroscopy, X-ray diffraction analysis, FTIR and X-ray photoelectron spectroscopy. The Mössbauer spectra were obtained at room temperature (RT) and liquid nitrogen temperature (LNT) with a Wissel electromechanical spectrometer operating in a constant acceleration mode (Wissenschaftliche Elektronik GmbH, Germany). A ^{57}Co/Rh (activity $\cong$ 50 mCi) source and an α-Fe standard were used. The conversion Mössbauer spectra were obtained at room temperature using CEMS Detector RiKon-5 and a helium/methane mixture. The experimentally obtained spectra were fitted by a mathematical procedure based on the least squares method. The parameters of hyperfine interaction such as isomeric shift (IS), quadrupole splitting (QS) and effective internal magnetic field (H_{eff}) as well as the line widths (FWHM) and the relative weight (G) of the partial components of the spectra were determined. Powder X-ray diffractometer (TUR-M62 apparatus, Germany) was used. It was equipped with a computer-controlled HZG-4 goniometer and the used radiation was Co-K_α. Phase identification was done according to JCPDS, Powder Diffraction File (PDF), Set 1–44, Joint Committee on Diffraction Standards, Philadelphia PA, USA, 1994.

FTIR spectra of the samples were recorded with spectrometer Nicolet 6700 FTIR (Thermo Electron Corporation, USA) in the middle region 400–4000 cm^{-1}. The materials were studied in diffuse-reflectance mode using Collector II accessory (Thermo Spectra-Tech, USA). 50 scans were used at spectra collection.

X-ray photoelectron measurements were carried out on the ESCALAB MkII (VG Scientific) electron spectrometer at a base pressure in the analysis chamber of 5×10^{-10} mbar using twin anode MgK_α/AlK_α X-ray source with excitation energies of 1253.6 and 1486.6 eV, respectively. The spectra were recorded at the total instrumental resolution (as it was measured with the FWHM of $Ag3d_{5/2}$ photoelectron line) of 1.06 and 1.18 eV for MgK_α and AlK_α excitation sources, respectively. The energy scale was calibrated by normalizing the C1s line to 285.0 eV. The processing of the measured spectra includes a subtraction of X-ray satellites and Shirley-type background [13]. The peak positions and areas are evaluated by a symmetrical Gaussian-Lorentzian curve fitting. The relative concentrations of the different chemical species are determined based on normalization of the peak areas to their photoionization cross-sections, calculated by Scofield [14].

2.3 Catalytic measurements

The catalytic tests were carried out in a flow type glass reactor at atmospheric pressure with a catalyst loading of about 0.8 cm^3 (fraction 0.25–0.31 mm). The gas mixture consists of 1 vol. % CO, 1 vol.% O_2, 50 vol. % H_2 and He for balance to 100 vol. %. External mass transfer limitations were minimized by working at high GHSV (18 750 h^{-1}). The reaction temperature was measured by an internal thermocouple. The gas analysis was performed by a HP5890 series II gas chromatograph equipped with a thermal conductivity detector and Carboxen-1000 column. Helium was used as a carrier gas. Alborg mass flow controllers were used for the control of the gas flow rates.

The CO conversion was calculated from the change of the CO concentration:

$$\mathbf{CO_{conversion}} = \mathbf{[CO]_{in}} - \mathbf{[CO]_{out}} \times \mathbf{100}/\mathbf{[CO]_{in}} \quad \%$$

The O_2 conversion was based on O_2 consumption:

$$\mathbf{O_{2conversion}} = \mathbf{[O_2]_{in}} - \mathbf{[O_2]_{out}} \times \mathbf{100}/\mathbf{[O_2]_{in}} \quad \%$$

Finally, the selectivity of the CO oxidation was calculated from the oxygen mass balance as follows:

$$\mathbf{Selectivity} = \mathbf{0.5} \times (\mathbf{[CO]_{in}} - \mathbf{[CO]_{out}}) \times \mathbf{100}/(\mathbf{[O_2]_{in}} - \mathbf{[O_2]_{out}}) \quad \%$$

All samples are reduced 1 h. at 300 °C in hydrogen flow before reaction.

The catalytic activity tests were performed up to temperature of 100 % conversion of oxygen. For different samples this temperature is different and depends on type of catalyst. 100 % conversion of O_2 means that all oxygen in the reaction mixture is used for oxidation reaction.

3 Results and discussion

The XRD patterns of activated carbon and all supported samples showed the characteristic pattern of the support only. This reveals that the supported metal or metal oxide phases are X-ray amorphous, because of the small crystallite size. No other phases are registered. X-ray diffraction pattern of used support activated carbon is shown on Fig. 1. The characteristic two diffraction peaks d_{002} and d_{100} can be seen on the picture, as well as the low intensity lines of Carbon (PDF 46-0945), Xylitol – $C_5H_{12}O$ (PDF 32-1981), and lines of traces of $Fe_5(PO_4)_4(OH)_3.2H_2O$ (PDF 45-1436) and $FeSiO_3$ (PDF 18-0877). The amorphous background is also presented in all recorded spectra. Figure 1 is an evidence that studied activated carbon has a turbostratic structure [15]. The turbostratic model assumes that the sample is made of graphite-like microcrystallites, bounded by cross linking network, consisting of several graphite-like layers, stacked nearly parallel and equidistant, with each layer having a random orientation. The size, mutual orientation and stacking of the microcrystallites are strongly associated with the porosity and the high surface area. The main characteristics of activated carbon determine its catalytic properties.

The obtained supported samples were studied using Mössbauer spectroscopy and the recorded spectra are shown on Fig. 2. Spectra evaluation was done as an optimal fit of component superposition. The spectra of samples reveal the presence of doublet components only. The calculated values of hyperfine parameters, the relative weights and FWHM after spectra evaluation are listed in Table 1. However phase identification gathered from doublet

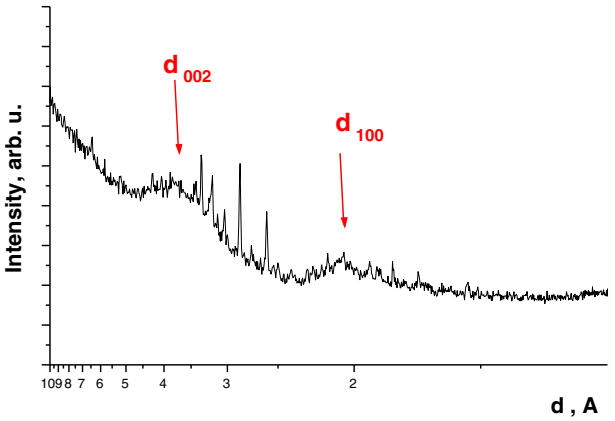

Fig. 1 X-ray diffraction patterns of activated carbon support

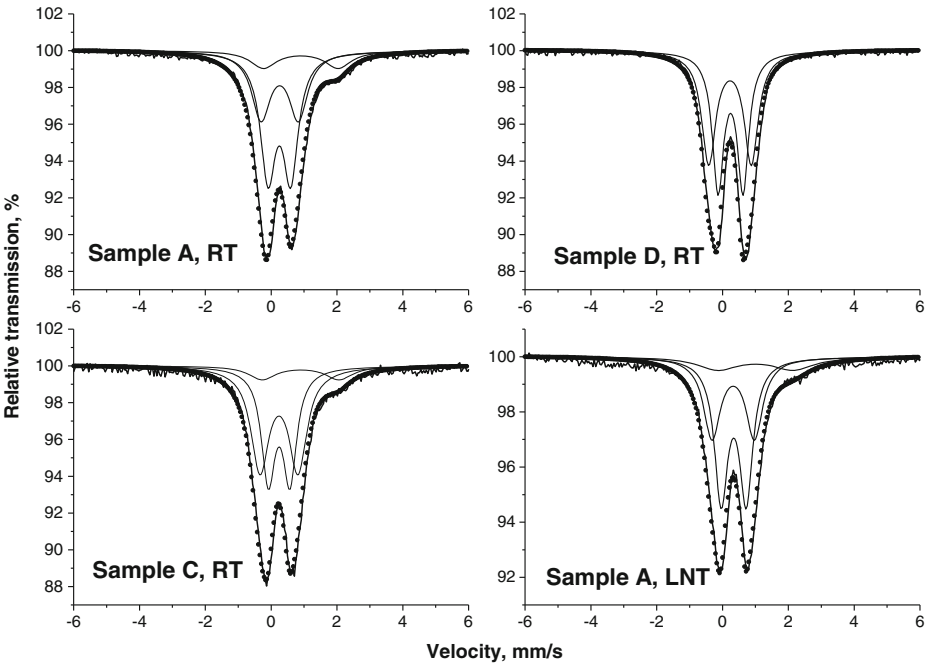

Fig. 2 Mössbauer spectra of: **Sample A** – RT, **Sample C** – RT, **Sample D** – RT and **d - Sample A** – LNT

type spectra should be carefully done. Since the samples are treated at temperatures exceeding the temperature of decomposition of the used precursor iron nitrate ($Fe(NO_3)_3.9H_2O$), the observed spectra are most probably due to iron oxide [16, 17]. The data from a variety of techniques indicated that very small supported particles can be prepared in this case such as one to a few atomic layers thick [studies listed in Ref. 9]. Both observations and theory indicate that in such thin magnetic materials "surface" behavior is expected [9]. Then the

Table 1 Calculated hyperfine parameters obtained from the fit of Mössbauer spectra carried out at room temperature and at 77 K

Sample	Components	IS, mm/s	QS, mm/s	FWHM, mm/s	G, %
Sample A	Db1	0.35	0.69	0.56	52
	Db2	0.36	1.13	0.68	38
	Db3	1.01	2.27	0.97	10
Sample A - LNT	Db1	0.44	0.76	0.49	51
	Db2	0.43	1.29	0.62	39
	Db3	1.10	2.35	1.50	10
Sample A - CEMS	Db1	0.31	0.68	0.47	58
	Db2	0.98	2.21	0.70	42
Sample C	Db1	0.34	0.66	0.50	49
	Db2	0.34	1.15	0.66	41
	Db3	0.97	2.33	1.00	10
Sample D	Db1	0.34	0.76	0.41	50
	Db2	0.33	1.29	0.51	50
Sample A after catalytic test	Db1	0.36	0.73	0.60	67
	Db2	0.37	1.23	0.63	21
	Db3	1.01	2.23	0.92	12
Sample C after catalytic test	Db1	0.36	0.75	0.57	72
	Db2	0.37	1.23	0.62	13
	Db3	1.03	2.18	0.97	15
Sample D after catalytic test	Db1	0.35	0.63	0.38	35
	Db2	0.34	1.01	0.41	33
	Db3	0.35	1.41	0.54	32

main impact in this case is the contribution of inner and surface part of iron oxide particle, rather than the impact of tetrahedrally/octahedrally coordinated iron ions (A sites and B sites, respectively). The A sites and B sites are not distinguishable as in the bulk case and Mössbauer analysis gives an overall doublet pattern which is defined as superparamagnetic structure [18]. The iron atoms on or near the particle surface exhibit somewhat different Mössbauer parameters from those in the particle interior [19]. The determined hyperfine parameters of the two sets of doublet lines (Dbl. 1 and Dbl. 2) can be assigned to preparation of supported ultradisperse iron oxide particles ($D < 10$ nm) with superparamagnetic behaviour due to thermally activated reversals of the particles magnetization (Table 1). In attempt to estimate the change of size of supported phase before and after catalytic tests, the core-shell model [19, 20] was applied for these two quadrupole doublets as belonging to iron ions from the "core" and the interface ("shell layers") of the nanoparticles. The doublet (Dbl. 1) with lowest $QS = 0.66 - 0.69$ mm/s belongs to iron ions from the "core" of the particles. The doublet (Dbl. 2) with larger $QS = 1.13 - 1.25$ mm/s can be assigned to interface (from the "shell" layers) ferric ions. The lower symmetry in the environment of the "surface" iron ions results in a change in the electric field gradient and therefore in a shift of the QS. Both QS values are higher than reported in [19]. But this can be explained by presence of support and inequivalent atomic environments for iron in the case of iron chemically impregnated into the coal [9–11, 20]. Two of experimentally obtained spectra of prepared

samples include the third doublet component also (Fig. 2). According to calculated parameters (Table 1) it can be assigned to the presence of Fe^{2+}-ions in non-equivalent positions. In order to characterize supported phase Mössbauer spectra at liquid nitrogen temperature (LNT) are registered. There are no other differences obtained instead of the characteristic ones for low temperature spectra parameters. In this reason only one of LNT spectra is presented (Fig. 2-b and Table 1). According to the literature data if iron oxide particles are SPM even at LNT, their size is below 4 nm [8, 10, 20]. As the surface of catalytic materials is the place of catalytically active centres, the conversion electron Mössbauer spectra (CEMS) are very appropriate for their investigation. It was registered higher content of about 32 % of Fe^{2+}-ions on catalyst surface of Sample A (Fig. 3 and Table 1).

The recorded Mössbauer spectra after PROX reaction registered a partial change of iron oxide particles. All calculated values can be seen on Table 1. The supported iron oxide phases preserve their SPM behaviour, but there is a difference in spectra components in all studied samples. Mono-component and consequently supported active phases preserve the number of components, but the ratio between "core" and "surface" iron ions increases. This can be explained with partial agglomeration of iron oxide particles [17, 20]. Despite the agglomeration of the iron oxide particles, their size remained still bellow 10 nm after PROX reaction. The quantity of presented Fe^{2+} component increases. In the case of sample impregnated simultaneously with Fe and Pt salts (sample D) completely different behavior was observed. The "core"/"surface" ratio is not significantly changed, but an additional doublet component appears in spectrum. According to calculated hyperfine parameters it can be associated both with an agglomeration of iron oxide particles or interaction between the active phases with formation of mixed oxide particles $PtFe_xO_y$ [6].

FTIR method had been widely used to characterize the surface groups of different oxides, and also applied to various types of carbon and carbonaceous materials. Since IR spectra had peaked shapes where the specific chemical bonds existed, it was possible to know which functionalities were created on the surface of activated carbon by comparing positions and intensity of the bands [21, 22].

Infrared spectra of the studied samples with active carbon support were recorded in diffuse–reflectance mode (Fig. 4). The band at 2311 cm^{-1} can be assigned to CO_2 adsorbed on the surface of active carbon [23]. The band at 1605 cm^{-1} is assigned to C–C vibration in dienes [22]. The region 1330–1280 cm^{-1} is characteristic about vibrations in OH groups [23]. Fe-O vibrations characteristic for magnetite appear at 474 and 561 cm^{-1} [16]. In related literature the bands registered at about 470, 565 and 670 cm^{-1} can be also assigned to C-H vibrations out of the plane in substituted aromatic compounds [21]. Comparative analysis of the collected spectra showed that the spectrum of sample Fe–AC is characterized with increased absorbance in this region and the band at 474 cm^{-1} is more intensive. This is in accordance with magnetite presented in the sample. The weak band positioned at about 1518 cm^{-1} together with the bands in the range 1000–1150 cm^{-1} observed in the spectra of samples AC, Sample A, Sample C and Sample D could be assigned to C-C vibrations in aromatic hydrocarbons [21–23]. Low intensity band observed at 2275 cm^{-1} in the spectra of samples AC, Sample B, Sample C and Sample D, despite it is not well outlined, can be assigned to C≡N vibrations [21–23]. Solely in the spectrum of sample D weak bands are registered in the interval 2900-3000 cm^{-1}. They can due to characteristic vibrations of CH and CH_2 groups in saturated hydrocarbons as well as to the presence of surface formates [21–23]. The broad band positioned at about 3500 cm^{-1} in the spectrum of Sample D is characteristic for vibrations of hydrogen bound OH groups on the surface of the sample [23].

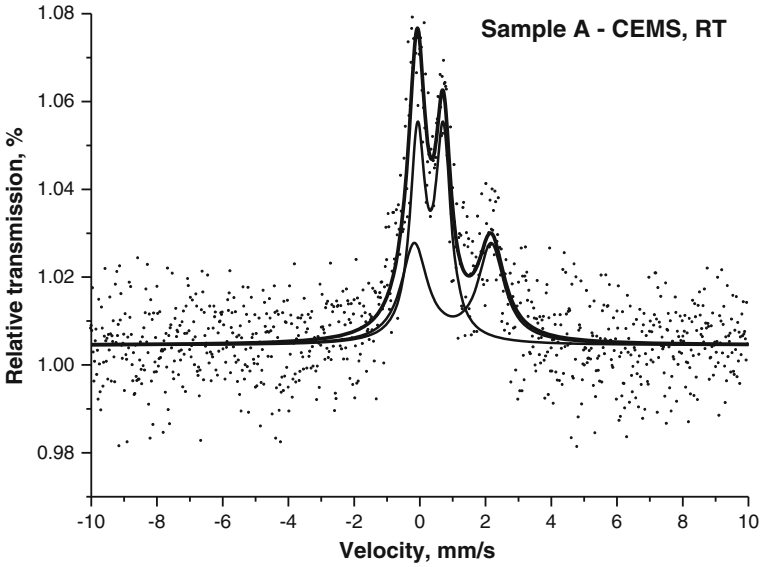

Fig. 3 Conversion electron Mössbauer spectrum of **Sample A** – RT

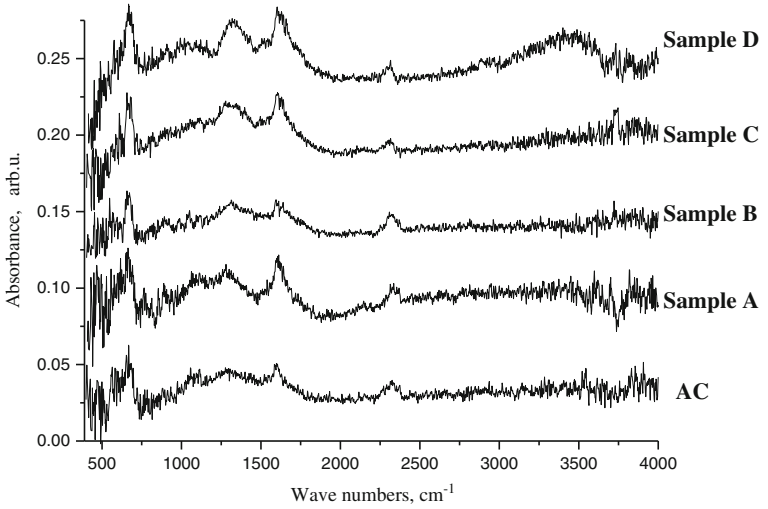

Fig. 4 FTIR spectra of activated carbon support (**AC**), **Sample A, Sample B, Sample C** and **Sample D**

The XRD and Mössbauer spectroscopy data were confirmed and completed by X-ray photoelectron spectroscopy (XPS) study of the samples. Moreover, the use of XPS method is particularly appropriate because it provides information about the chemical composition and surface functionalities of carbon material solid surfaces [24]. This technique is widely used for investigation of catalytic samples before and after catalytic tests. It provides information of possible changes in the chemical states of the deposited catalytic particles. Using

Table 2 Surface atomic concentration of elements (at. %) presented on the surface of the studied samples

	C1s	O1s	Fe2p	Pt4f	K2p	Ca2p	N1s	P2p	Si2s
Sample A	57	26	8	0	1	3	0	4	2
Sample B	84	10	0	0.1	2	1	0	2	0
Sample C	59	24	5	0.1	1	3	1	4	2
Sample D	54	26	8	0.1	1	2	< 1	6	1

survey and high resolution spectra of the samples we were able to calculate the atomic concentration of all elements presented on the surface (Table 2). The lack of peaks in the zones of binding energies characteristic for the presence of nitrate and chloride ions enables us to claim that the chosen synthesis conditions are suitable for complete transformation of the deposited salts into supported active phases. Table 2 shows that the surface consists basically of carbon and oxygen, mixed with potassium, nitrogen, silicon, calcium and phosphorus. These elements are typical for active carbon used as a support as revealed by our investigation before the impregnation of the active phase of iron, platinum and mixed iron-platinum catalysts.

Some of the most informative high resolution XP spectra, as well as the result of peak component analysis are shown in Fig. 5. Figure 5a includes XP spectra of C1s and K2p core levels shown for Sample D, but the same spectra are obtained for other samples as well.

The surface of the active carbon support consists of several chemical carbon groups. Figure 5a represents the curve fitting procedure of the C1s spectrum, which shows the presence of C≡C (1), C-C, C-H (2), C-O, C-N (3), C=O, C-OOH, OH, COH, N-O-C (4) and O-C=O, $OH_{ads.}$, O_{2ads} (5) chemical groups [24–26]. These forms of carbon, together with their binding energies are shown in Table 3. The corresponding binding energies measured for oxygen, also given in Table 3, are obtained by similar curve fitting procedure shown in Fig. 5b. The peaks marked with 2, 3, 4 and 5 in Fig. 5b are raleted to chemical groups C-O, C-N, C=O, C-OOH, OH, COH, N-O-C and O-C=O, $OH_{ads.}$, O_{2ads}, respectively. Their binding energies are given conveniently against the binding energies of carbon in Table 3. The lowest in intensity peak, marked with 1 in Fig. 5b with binding energy of about 529.8 eV is related to the metal oxides of the deposited phase of Fe, Pt and Fe-Pt catalysts for all samples.

Fe2p XP spectra of the deposited iron-oxide phase on AC for Sample A, Sample C and Sample D are shown on Fig. 5c. The line form, position of the peak as well as the position of satellite structures are characteristic for the oxidation state of the iron. Comparison with previously registered iron oxide spectra and with literature data also, shows the presence of Fe_3O_4 as a main phase in all samples [27]. For the Sample D we have observed line form which is very close to the line form of Fe measured from Fe_3O_4 sample. For Sample A and Sample C, we observe some deviations from the line form measured for Fe_3O_4. Namely, we observe very weak satellite structures at binding energies about 719 eV (typical for Fe^{3+}) and about 714 eV (typical for Fe^{2+}). The relative areas are close to the characteristic ones for the magnetite phase in Sample D, but in Samples A and C the quantity of Fe^{3+} are greater. The broadening of Fe2p peaks corresponds to the presence of nano-sized particles. Therefore, one can think that on the surface of the AC exist well dispersed nano-sized iron-oxide particles, which are consistent of Fe_3O_4 core covered mainly with Fe^{3+} ions.

Together with iron oxides for some of the samples we used also platinum as an active phase. Figure 5d shows a spectrum of Pt4f (Sample B) with its components obtained by

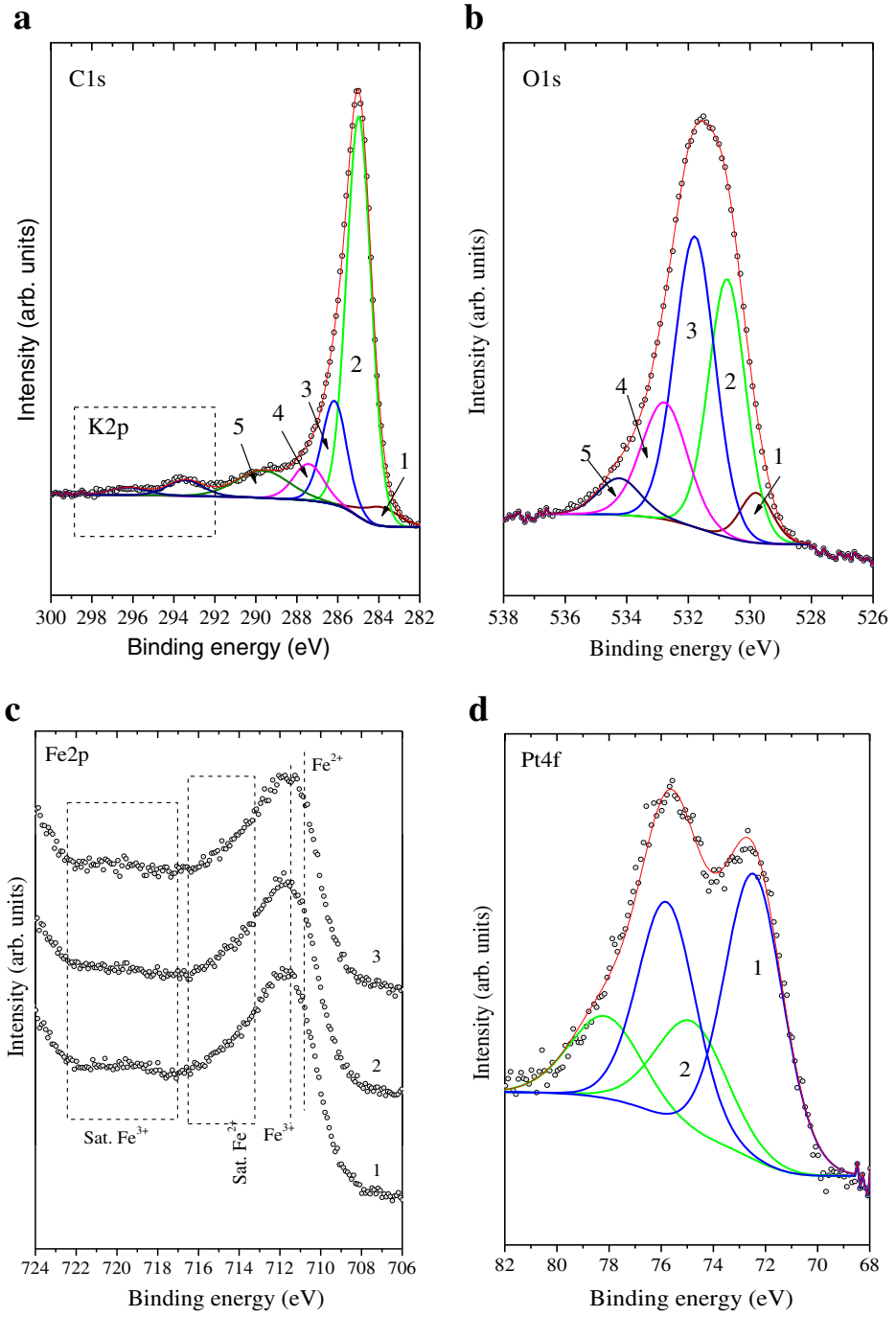

Fig. 5 XPS spectra of samples

Table 3 Active carbon support chemical groups and their binding energies obtained by curve fitting procedure for C1s and O1s peaks

Chemical groups	C1s, BE, eV	O1s, BE, eV
C≡C	283.6	-
C-C, C-H	285.0	-
C-O, C-N	286.2	533.1
C=O, C-OOH, OH, COH, N-O-C	288.0	534.6, 531.7
O-C=O, $OH_{ads.}$, O_{2ads}	290.5	536.5

curve fitting procedure. The line form and the curve fitting procedure reveal that the platinum exists in two forms, i.e., metal platinum Pt^0 with binding energy of about 72.4 eV and oxidized platinum Pt^{2+} with binding energy of about 74.8 eV. The registered shift of about 1 eV in BE is due to the nano-metric size of particles. Similar procedure is applied for the other two containing Pt samples (C and D). Based on the curve fitting procedure we have estimated the ratio between Pt^{2+} and Pt^0. For Sample B we have calculated $Pt^{2+}/Pt^0 = 0.470$, whereas for Sample C and D the ratio is 0.639 and 0.408, respectively.

The chemical analysis of XPS has been extended with the model proposed by Kerkhof-Moulijn in 1979 [28] and simplified by Leon in 1995 [29]. These models are based on the description of catalyst as layers of the carrier with the active phase, well dispersed on it. They can be used for evaluating the size of nanoparticles of the deposited active phase on the support. The prepared samples include well dispersed magnetite and platinum, platinum-oxides promoter phase, which deviates from the monolayer deposition on the support of active carbon. This representation gives us the ability to use a simplified Kerkhof-Moulijn model [29] and numerical recipe described by Kolev and Tyuliev [30] for estimating the mean effective size of the catalyst nanoparticles. Calculated particle size of Fe_3O_4 varies in the values of 0.5–2 nm. This result is in a very good agreement with those found by the Mössbauer study (bellow 4 nm). Calculated particle size of platinum is about 7–8 nm. Both of used models ("core-sell" and Kerkhof-Moulijn model) give no absolute values of mean particle size, but they are very appropriate for comparison of samples series. This gives the possibility to compare the change of prepared supported phases during the catalytic measurements.

The O_2 and CO conversion and CO_2 selectivity curves are shown on Figs. 6, 7 and 8. A one-component platinum catalyst (Sample B) is the most active and selective at the studied reaction temperatures. The selectivity to carbon dioxide for Sample B increases with temperature and reaches maximum of 40 %. Catalytic activity in CO conversion decrease with Fe loading and this is more noticeable for a sample prepared by common solution of platinum and iron nitrates. For all samples modified with Fe selectivity to CO_2 decreases with temperature increase. This means that at low temperature oxygen preferentially interacts with CO, but at higher temperatures reacts with hydrogen. Catalytic behavior of iron modified samples is quite surprising considering a numerous literature data according which the modification of platinum with iron significantly increases the activity in PROX reaction [1, 2, 31–33]. It was suggested that the promoting effect of iron oxide in the case of Pt-Fe catalysts is related to the ability of the iron oxide species, located in close proximity to platinum, to provide adsorption sites for oxygen that can subsequently react with CO molecules adsorbed on adjacent Pt sites through a noncompetitive dual site mechanism [1, 2]. One of possible explanation for a low activity of our two-component Pt-Fe samples is a higher concentration of iron oxide on the support. S. Kandoi *et al.* [34] studied the selective oxidation

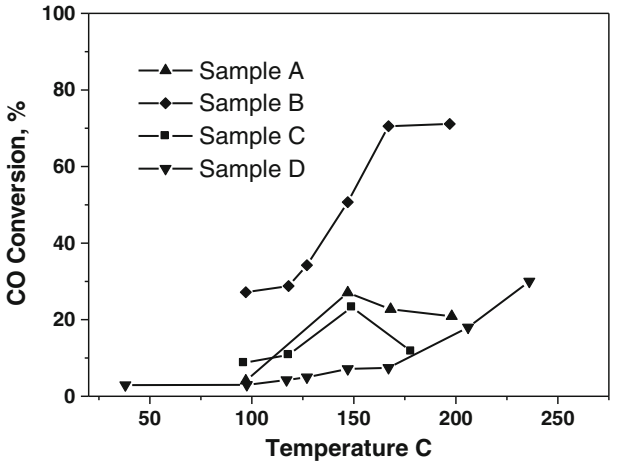

Fig. 6 CO conversion with temperature

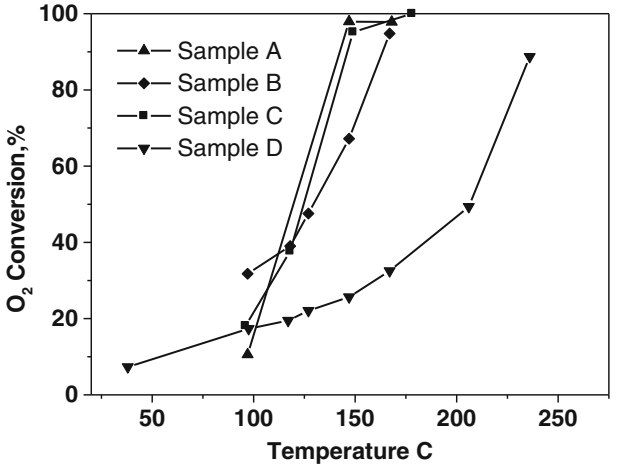

Fig. 7 O_2 conversion with temperature

of CO with respect to H_2 on Pt(111) by using the periodic, self-consistent and DFT calculations. These authors show a higher activation energy barrier for CO oxidation (0.96 eV) than H_2 oxidation (0.83 eV) on Pt(111). The iron oxide is predominant active phase in our bicomponent samples leading to the increasing in surface oxygen species. The combination of both factors the lower activation energy for the oxidation of H_2 and a high concentration of active oxygen at the surface of the iron containing phase is a possible explanation for the low selectivity to CO_2 of the iron modified catalysts. The XPS data for the bimetal catalyst with the lower activity are in accordance with this statement. As it can be seen from Table 2, the ratio Fe/Pt is higher on the surface of catalysts prepared by common solution (Sample D).

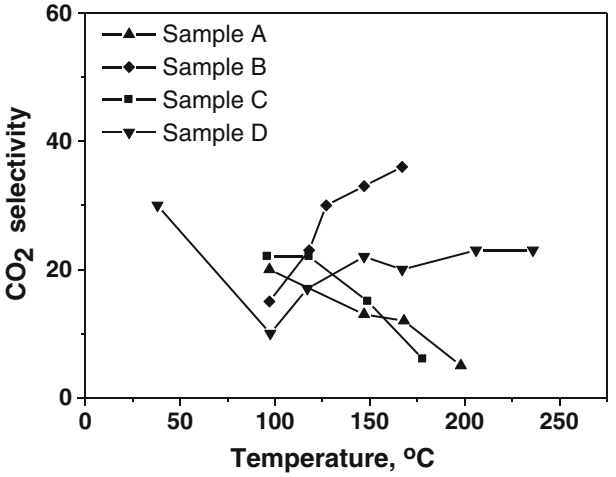

Fig. 8 CO_2 selectivity with temperature

4 Conclusions

The used preparation conditions result in synthesis of iron and iron-platinum catalysts supported on activated carbon. Characterization of materials show the presence of iron oxide (Fe_3O_4) as a main supported phase in iron containing samples (A, C and D) and Pt and PtO in platinum containing samples (B, C and D). The mean effective particle size of supported phases was calculated in order to compare the change of prepared supported phases before and after catalytic tests. The Mössbauer, IR and XPS results show that the activated carbon support and the preparation procedure give rise to the synthesis of isolated metal Pt ions and ultradispersed Fe and Pt oxide species. Probably the presence of different functional groups of activated carbon (studied by XPS) gives rise to registered very high dispersion of loaded species on support.

The catalytic performance of mono- and bi-component iron/platinum catalyst was tested in PROX reaction. It was established that catalytic behaviour of studied materials depends on their phase composition and dispersity. A lower activity of two-component Pt-Fe samples in comparison with one-component Pt one, was explained with the increase in surface oxygen species as result of predomination of iron oxide on the support leading to the increase in selectivity to the H_2 oxidation. Partial agglomeration of supported iron oxide phase was registered.

Acknowledgments The authors are grateful for the financial support of National Science Fund of Bulgaria under Project DFNI-E 01/7/2012. The help of Dr G. Kadinov from the Institute of Catalysis of Bulgarian Academy of Sciences in discussion and interpretation of infrared spectra is greatly acknowledged.

References

1. Kotobuki, M., Watanabe, A., Uchida, H., Yamashita, H., Watanabe, M.J.: Reaction mechanism of preferential oxidation of carbon monoxide on Pt, Fe, and Pt.Fe/Mordenite catalysts. J. Catal. **236**, 262–269 (2005)

2. Liu, X., Korotkikh, O., Farrauto, R.: Structural study of the selective catalytic oxidation of CO in hydrogen. Appl. Catal. A Gen. **226**, 293–303 (2002)
3. Guczi, L., Petë, G., Beck, A., Pàszti, Z.: Electronic structure and catalytic properties of transition metal nanoparticles: the effect of size reduction. Top. Catal. **29**, 129–138 (2004)
4. Guczi, L.: Bimetallic nano-particles: featuring structure and reactivity. Chem. Inform., 36 (2005)
5. Bachiller-Baeza, B., Guerrero-Ruiz, A., Rodriguez-Ramos, I.: Role of the residual chlorides in platinum and ruthenium catalysts for the hydrogenation of α,β-unsaturated aldehydes. Appl. Catal. A Gen. **192**, 289–297 (2000)
6. Waychunas, G., Kim, C., Banfield, J.: Nanoparticulate iron oxide minerals in soils and sediments: unique properties and contaminant scavenging mechanisms. J. Nanopart. Res. **7**, 409–433 (2005)
7. Johnson, C.E., Costa, L., Gray, S., Johnson, J.A., Krejci, A.J., Hasan, S.A., Gonzalo-Juan, I., Dickerson, J.H.: Mössbauer measurements on spinel-structure iron oxide nanoparticles. In: Proceedings 36th Annual Condensed Matter and Materials Meeting, pp. FO01:1–FO01:6. Wagga Wagga (2012)
8. Bødkert, F., Mørup, S., Oxborrow, C.A., Linderoth, S., Madsen, M.B., Niemansverdriet, J.W.: Mössbauer studies of ultrafine iron-containing particles on a carbon support. J. Phys. Condens. Matter **4**, 6555–5568 (1992)
9. Phillips, J.: Application of Mössbauer spectroscopy for the characterization of iron-containing catalysts. Hyperfine Interact. **111**, 3–16 (1998)
10. Jung, H.-J., Vannice, M., Mulay, L., Stanfield, R., Delgass, W.: The characterization of carbon-supported iron catalysts: chemisorption, magnetization, and Mössbauer spectroscopy. J. Catal. **76**, 208–224 (1982)
11. Ganguly, B., Huggins, F.E., Rao, K.R.P.M., Huffman, G.P.: Determination of the particle-size distribution of iron oxide catalysts from superparamagnetic Mössbauer relaxation spectra. J. Catal. **142**(2), 552–560 (1993)
12. Paneva, D., Jovanović, D., Tsoncheva, T., Matić, L., Kunev, B., Terlecki-Baričević, A., Mitov, I., Minchev, C.: Bulg. Chem. Commun. **34**, 384–394 (2002)
13. Shirley, D.: High-resolution x-ray photoemission spectrum of the valence bands of gold. Phys. Rev. B **5**, 4709–4714 (1972)
14. Scofield, J.H.: Hartree-Slater subshell photoionization cross-sections at 1254 and 1487 eV. J. Electron. Spectrosc. Relat. Phenom. **8**, 129–137 (1976)
15. Coutinho, A.R., Rocha, J.D., Luengo, C.A.: Preparing and characterizing biocarbon electrodes. Fuel Process. Technol. **67**, 93–102 (2000)
16. Cornell, R.M., Schwertmann, U.: The Iron Oxides. Structure, Properties, Reactions, Occurrences and Uses, Second Completely Revised and Extended Edition. Wiley-VCH Verlag GmbH and Co KGaA, Weinheim (2003)
17. Dumesic, J., Topsoe, H.: Mössbauer spectroscopy applications to heterogeneous catalysis. Adv. Catal. **26**, 121–246 (1977)
18. Chuev, M.: Mössbauer spectra of single-domain particles in a weak magnetic field. J. Phys. Condens. Matter. **20**, 505201-(10pp) (2008)
19. Van Der Kraan, A.: Mössbauer effect studies of surface ions of ultrafine α-Fe_2O_3 particles. Phys. Status Solidi A **18**, 215–226 (1973)
20. Niemantsverdriet, J.W., Van der Kraan, A.M., Delgass, W.N., Vannice, M.A.: Small-particle effects in Mössbauer spectra of a carbon-supported iron catalyst. J. Phys. Chem. **89**, 67–72 (1985)
21. Zawadzki, J.: Infrared spectroscopy in surface chemistry of carbons. In: Thrower, P.A. (ed.) Chemistry and Physics of Carbon, pp. 147–386. Marcel Dekker, New York (1988)
22. Fanning, P.E., Vannice, M.A.: A DRIFTS study of the formation of surface groups on carbon by oxidation. Carbon **31**, 721–730 (1993)
23. Little, L.H.: Infrared Spectra of Adsorbed Species. Academic Press Inc. Ltd., New York (1966)
24. Sherwood, M.A.P.: Surface analysis of carbon and carbon fibers for composites. J. Electron. Spectrosc. Relat. Phenom. **81**, 319–342 (1996)
25. Burke, G., Wurster, D., Berg, M., Veng-Pedersen, P., Schottelius, D.: Surface characterization of activated charcoal by X-Ray Photoelectron Spectroscopy (XPS): correlation with phenobarbital adsorption data. Pharm. Res. **9**(1), 126–130 (1992)
26. Shen, W., Li, Z., Liu, Y.: Surface chemical functional groups modification of porous carbon. Recent Patents Chem. Eng. **1**, 27–40 (2008)
27. Gota, S., Guiot, E., Henriot, M., Gautier-Soyer, M.: Atomic-oxygen-assisted MBE growth of a-Fe_2O_3 on a-Al_2O_3(0001): Metastable FeO(111)-like phase at subnanometer thicknesses. Phys. Rev. B **60**(20) (1999)
28. Kerkhof, F.P.J.M., Moulijn, J.A.: J. Phys. Chem. **83**, 1612–1619 (1979)
29. Leon, V.: A simplified Kerkhof-Moulijn model for dispersion quantification from XPS atomic concentrations. Surf. Sci. **339**, L931–L934 (1995)

30. Kolev, H., Tyuliev, G.: Quantitative XPS applied to nanostructures study. In: Balabanova, E., Dragieva, I. (eds.) Nanoscience & Nanotechnology, vol. 9, pp. 84–87. Heron Press, Sofia (2009)
31. Kotobuki, M., Watanabe, A., Uchida, H., Yamashita, H., Watanabe, M.: High catalytic performance of Pt-Fe alloy nanoparticles supported in mordenite pores for preferential CO oxidation in H_2-rich Gas. Appl. Catal. A Gen. **307**, 275–283 (2006)
32. Watanabe, M., Uchida, H., Ohkubo, K., Igarashi, H.: Hydrogen purification for fuel cells: selective oxidation of carbon monoxide on Pt-Fe/Zeolite catalysts. Appl. Catal. B Environ. **46**, 595–600 (2003)
33. Roberts, G., Chin, P., Sun, X., Spivey, J.: Preferential oxidation of carbon monoxide with Pt/Fe monolithic catalysts: interactions between external transport and the reverse water-gas-shift reaction. Appl. Catal. B Environ. **46**, 601–611 (2003)
34. Kandoi, S., Gokhale, A.A., Grabow, L.C., Dumesic, J.A., Mavrikakis, M.: Why Au and Cu are more selective than Pt for preferential oxidation of CO at low temperature. Catal. Lett. **93**, 93–100 (2004)